NASA TN D-1786

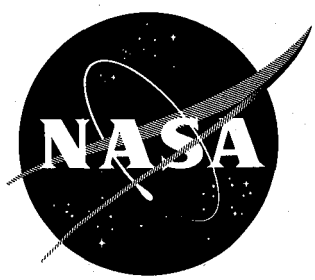

TECHNICAL NOTE

D-1786

STATIC AERODYNAMIC CHARACTERISTICS OF A THREE-STAGE ROCKET VEHICLE HAVING VARIOUS FIN CONFIGURATIONS AT LOW SUBSONIC MACH NUMBERS AND ANGLES OF ATTACK UP TO 28°

By Clarence A. Brown, Jr., and Lawrence E. Putnam

Langley Research Center
Langley Station, Hampton, Va.

NATIONAL AERONAUTICS AND SPACE ADMINISTRATION

WASHINGTON

April 1963

NATIONAL AERONAUTICS AND SPACE ADMINISTRATION

TECHNICAL NOTE D-1786

STATIC AERODYNAMIC CHARACTERISTICS OF A THREE-STAGE ROCKET VEHICLE HAVING VARIOUS FIN CONFIGURATIONS AT LOW SUBSONIC MACH NUMBERS AND ANGLES OF ATTACK UP TO 28°

By Clarence A. Brown, Jr., and Lawrence E. Putnam

SUMMARY

The subsonic static aerodynamic characteristics of a 0.081- or 1/12.4-scale model of the Trailblazer II three-stage rocket vehicle were determined in the Langley low-turbulence pressure tunnel for application to the calculation of wind effects on vehicle trajectories. Included is a study of the effect of fin size and aspect ratio on the aerodynamic characteristics of the vehicle. The tests were made at Mach numbers near 0.2, at Reynolds numbers per foot from 7.06×10^6 to 9.01×10^6, and at angles of attack up to approximately 28°. Aerodynamic moments were taken about a point 34.555 inches (0.692 of the body length) aft of the model nose. This point corresponds to the center-of-gravity location of the loaded full-scale Trailblazer II configuration.

The results showed that reducing the fin size at a fixed aspect ratio caused a decrease in lift and drag coefficients throughout the angle-of-attack range of the present investigation and a decrease in stability below an angle of attack of about 14°. Decreasing the fin aspect ratio at constant fin area resulted in a decrease in lift coefficient and stability below an angle of attack of about 14°. The results also show that all fin configurations were statically stable below an angle of attack of 14°, but that the configuration with fins of low aspect ratio and small area would be the least sensitive to ground winds at launch.

INTRODUCTION

The National Aeronautics and Space Administration, in conjunction with the Massachusetts Institute of Technology Lincoln Laboratory, is currently investigating reentry physics phenomena by the use of rocket vehicles launched from NASA Wallops Station. One of the rocket vehicles used in this investigation is a fin-stabilized three-stage solid-fuel configuration known as the Trailblazer II. The vehicle is unguided and hence it is necessary to exercise all available means for minimizing vehicle-impact dispersion for both range safety and data acquisition

purposes. Inasmuch as the atmospheric wind velocity is one of the more significant causes of vehicle impact dispersion, it is necessary to adjust the vehicle launch angles to compensate for the wind effects. Methods are available, such as that of reference 1, for determining wind effects on vehicle trajectories; however, these methods require a knowledge of the vehicle aerodynamic characteristics. References 2 and 3 contain aerodynamic information on the Trailblazer II configuration measured in wind-tunnel tests made at supersonic speeds. The present paper is concerned with similar tests made at low speeds. These low-speed tests have been found necessary because the greatest wind effects are experienced at low altitudes before the vehicle has accelerated to high speed.

The tests reported herein were made in the Langley low-turbulence pressure tunnel on an 0.081- or 1/12.4-scale model of the Trailblazer II configuration to determine its static stability at low speeds. The effect on the static stability of reducing the tail fin area at both the design aspect ratio and at a reduced aspect ratio was also investigated. The tests were made over an angle-of-attack range from approximately -4° to 28° at Mach numbers near 0.2. The Reynolds numbers per foot ranged from 7.06×10^6 to 9.01×10^6.

SYMBOLS

The coefficients of forces and moments are referred to the body-axis system illustrated in figure 1. Aerodynamic moments are taken about a point located 34.555 inches (0.692 vehicle length) aft of the model nose. This moment center corresponds to the center-of-gravity location of the loaded full-scale Trailblazer II configuration. Symbols used in this paper are as follows:

A exposed fin aspect ratio

C_l rolling-moment coefficient, $\frac{\text{Rolling moment}}{qSd}$

C_m pitching-moment coefficient, $\frac{\text{Pitching moment}}{qSd}$

C_N normal-force coefficient, $\frac{\text{Normal force}}{qS}$

C_n yawing-moment coefficient, $\frac{\text{Yawing moment}}{qSd}$

C_Y side-force coefficient, $\frac{\text{Side force}}{qS}$

C_A axial-force coefficient, $\frac{\text{Axial force}}{qS}$

C_D drag coefficient, $C_A \cos \alpha + C_N \sin \alpha$

C_L	lift coefficient, $C_N \cos \alpha - C_A \sin \alpha$
d	diameter of first stage of test configuration, 2.501 in.
M	free-stream Mach number
q	free-stream dynamic pressure, lb/sq ft
S	cross-sectional area of first stage of test configuration, 0.03416 sq ft
α	angle of attack of model center line, deg
β	angle of sideslip of model center line, deg
R	Reynolds number per foot

MODELS

Photographs of the three-stage Trailblazer II configuration model are shown in figure 2. A two-view drawing with dimensional details of the model tested is presented in figure 3. The 0.081-scale model consisted of the first-stage booster with auxiliary rocket motors, the second-stage booster, and the velocity package of the Trailblazer II configuration.

The first-stage booster was equipped with cruciform modified double-wedge-shaped fins with leading-edge sweep of 18°24'. Three sets of fins, which are illustrated in figure 4, were provided for this first stage. One set represented the standard full-scale fins with an exposed area (outboard of the body) of 12 square feet per panel and an aspect ratio of 1.5. A second set, for which the fin shape was obtained by clipping the tips from the first fin design, represented full-scale fins with an exposed area of 10 square feet per panel and an aspect ratio of 0.985. The third set of fins represented full-scale fins with an exposed area of 10 square feet per panel and an aspect ratio of 1.5. For convenient reference, the fin configurations are identified herein as the 12-sq-ft, A = 1.5 fins; the 10-sq-ft, A = 0.985 fins; and the 10-sq-ft, A = 1.5 fins. The first-stage booster also had two auxiliary rocket motors mounted on the side. Sketches of these motors, along with the adapter used to connect the first- and second-stage boosters, are shown in figure 5.

The second-stage booster was equipped with cruciform wedge-shaped fins with a leading-edge sweep angle of 30°. These fins were alined with the first-stage booster fins. The wedge half-angle for these fins was 4° and the fins were 0.081 scale of the vehicle 4-sq-ft fins. A dimensional sketch of the model fins provided for the second-stage booster is shown in figure 5.

The nose of the velocity package is a hemispherical segment tangent to a 17° cone frustum. Another cone frustum of approximately 1° half-angle forms the tube section of the velocity package. The maximum diameter of the velocity

package is larger than that of the second-stage booster, so that an inverse cone-frustum adapter is used to connect these stages.

APPARATUS AND TESTS

The tests were made in the Langley low-turbulence pressure tunnel in which the test section is 3 by 7.5 feet. For these tests, forces and moments were measured by means of an internal six-component strain-gage balance which was sting supported in the tunnel. The tunnel can accommodate tests in air at stagnation pressures from 1 to 10 atmospheres at Mach numbers up to 0.4.

The tests were made at tunnel stagnation pressures of about 120 lb/sq in. abs and 72 lb/sq in. abs with corresponding Reynolds numbers per foot of about 9.0×10^6 and 7.0×10^6, respectively. All configurations were tested at Mach numbers near 0.2 and at angles of attack from approximately -4° to 28.5°.

All the tests of the present investigation were run with fixed transition in order to avoid changes in aerodynamic forces due to changes in the extent of laminar flow on the model. (See ref. 4.) An annular roughness strip 0.1 inch wide was installed 1.28 inches rearward of the model nose by blowing 0.003- to 0.004-inch-diameter carborundum grains on a thin layer of wet shellac.

All tests were made with the fins of the first-stage booster alined in the vertical and horizontal planes. (See fig. 3.) The two auxiliary rocket motors located on the first-stage booster would then be positioned in the upper left and lower right quadrants when the vehicle is viewed from the rear. The fin cant angle of both the first- and second-stage fins was set at zero.

ACCURACY AND CORRECTIONS

Estimated accuracy of the coefficients (based on balance accuracy), Mach number, and angle of attack is indicated as follows:

C_N	±0.1
C_A	±0.01
C_m	±0.2
C_l	±0.02
C_n	±0.08
C_Y	±0.1
M	±0.001
α, deg	±0.1

The axial-force data have been adjusted to a condition of free-stream static pressure at the model base. Jet-boundary corrections and tunnel-blockage corrections, as determined by methods of references 5, 6, and 7, have been applied to

the data. The angle of attack has been corrected for sting and balance deflections due to aerodynamic loads.

RESULTS AND DISCUSSION

The longitudinal aerodynamic characteristics for the model are presented in figures 6 to 9. The effect of a decrease in Reynolds number from 9.01×10^6 to 7.06×10^6 on the static longitudinal aerodynamic characteristics of the configuration with the 12-sq-ft, A = 1.5 fins has been evaluated from a study of the data presented in figures 6 and 7. As would be expected, there is very little effect from this small decrease in Reynolds number.

The effect of fin size on the static longitudinal aerodynamic characteristics of the configuration has been evaluated by comparing the data of figures 7 and 8. The lift, normal-force, and pitching-moment coefficients for both the 12-sq-ft, A = 1.5 fins and the 10-sq-ft, A = 1.5 fins were generally linear up to an angle of attack of about 14°, where separation or fin stall resulted in an unstable pitch-up. Generally, reducing the fin size resulted in a decrease in lift and drag coefficients for the angle-of-attack range of the present investigation. Although the configurations with both fin sizes were statically stable below an angle of attack of about 14°, a reduction in the fin size resulted in a decrease in stability. This change in fin size reduced the static margin from -1.8 to -1.4 body diameters, which is equivalent to a forward shift in the aerodynamic center from 39 inches to 38 inches aft of the model nose. Figure 10 shows that, as would be expected, reducing the fin size also caused the center of pressure to move forward for all angles of attack.

The effect of fin aspect ratio on the static longitudinal aerodynamic characteristics has been evaluated by comparing the data of figures 8 and 9. Decreasing the aspect ratio resulted in an increase in the angle of attack at which stall and associated pitch-up occurred from about 14° to about 16°. Up to an angle of attack of about 14°, a reduction in the aspect ratio resulted in a decrease in lift coefficient and a decrease in stability. The static margin for the fin configurations with A = 1.5 was -1.417d which corresponds to 38.10 inches aft of the model nose, and the static margin for the fin with A = 0.985 was -0.9576d which corresponds to 36.95 inches aft of the model nose. The center of pressure (fig. 10) also moved forward with a decrease in aspect ratio up to an angle of attack of about 14°. Between angles of attack of 14° and 22° this trend reverses and a decrease in fin aspect ratio resulted in an increase in lift coefficient (figs. 8 and 9) and a rearward movement of the center of pressure. Above an angle of attack of 22° the reduction in aspect ratio had essentially no effect on the aerodynamic characteristics of the configuration. Also the reduction in aspect ratio had essentially no effect on drag coefficient throughout the angle-of-attack range.

Although all fin configurations were statically stable below an angle of attack of about 14° (figs. 7, 8, and 9), the 10-sq-ft, A = 0.985 fin configuration had the least amount of stability and the lowest lift-curve slope. Therefore, for the full-scale vehicle the fin with the low aspect ratio and the small

area will be the least sensitive of the configurations tested to crosswinds during launch.

Figure 11 shows the lateral aerodynamic characteristics with angle of attack for all three configurations. Inasmuch as all tests were conducted at $\beta = 0^{\circ}$, these plots are presented to enable the reader to see the total forces and moments for the various configurations. None of the configurations experienced any appreciable buildup in rolling moment until the break in the pitching moment occurred. This buildup in rolling moment, after the break in the pitching-moment curve, is probably due to the auxiliary rocket rotors mounted on the first stage. The yawing moment was nearly linear with angle of attack until the break in the pitching moment occurred.

CONCLUSIONS

The subsonic static aerodynamic characteristics of a 0.081- or 1/12.4-scale model of the Trailblazer II three-stage rocket vehicle were determined in the Langley low-turbulence pressure tunnel for application to the calculation of wind effects on vehicle trajectories. Included is a study of the effect of fin size and aspect ratio on the aerodynamic characteristics of the vehicle. The investigation was made at Mach numbers near 0.2, at Reynolds numbers per foot from 7.06×10^6 to 9.01×10^6, and at angles of attack up to approximately 28°. Aerodynamic moments were taken about a point 34.555 inches aft of the model nose. This point corresponds to the center of gravity of the loaded full-scale Trailblazer II configuration. The results of the investigation indicate the following conclusions:

1. Decreasing fin size at a fixed aspect ratio resulted in a decrease in lift coefficient and drag coefficient throughout the angle-of-attack range of the investigation and in a decrease in stability below an angle of attack of approximately 14°.

2. Decreasing aspect ratio at constant fin area resulted in a decrease in lift coefficient and stability below an angle of attack of about 14°.

3. All fin configurations tested were statically stable.

4. Because the configuration with fins of low aspect ratio and small area had the least amount of stability and the lowest lift-curve slope, it would be the least sensitive to crosswinds during launch.

Langley Research Center,
National Aeronautics and Space Administration,
Langley Station, Hampton, Va., February 8, 1963.

REFERENCES

1. James, Robert L., Jr. (with Appendix B by Norman L. Crabill): A Three-Dimensional Trajectory Simulation Using Six Degrees of Freedom With Arbitrary Wind. NASA TN D-641, 1961.

2. Carraway, Ausley B., Edwards, Frederick G., and Keating, Jean C.: Investigation of the Static Stability Characteristics of Two Stages of a Three-Stage Missile at a Mach Number of 4.00. NASA TN D-651, 1961.

3. Brown, Clarence A., Jr., and Carraway, Ausley B.: Static Aerodynamic Characteristics of a Two-Stage and a Three-Stage Rocket Vehicle at Mach Numbers From 1.47 to 4.63. NASA TN D-1232, 1962.

4. Braslow, Albert L., and Knox, Eugene C.: Simplified Method for Determination of Critical Height of Distributed Roughness Particles for Boundary-Layer Transition at Mach Numbers From 0 to 5. NACA TN 4363, 1958.

5. Katzoff, S., and Hannah, Margery E.: Calculation of Tunnel-Induced Upwash Velocities for Swept and Yawed Wings. NACA TN 1748, 1948.

6. Swanson, Robert S., and Toll, Thomas A.: Jet-Boundary Corrections for Reflection-Plane Models in Rectangular Wind Tunnel. NACA Rep. 770, 1943. (Supersedes NACA WR L-458.)

7. Herriot, John G.: Blockage Corrections for Three-Dimensional-Flow Closed-Throat Wind Tunnels, With Consideration of the Effect of Compressibility. NACA Rep. 995, 1950. (Supersedes NACA RM A7B28.)

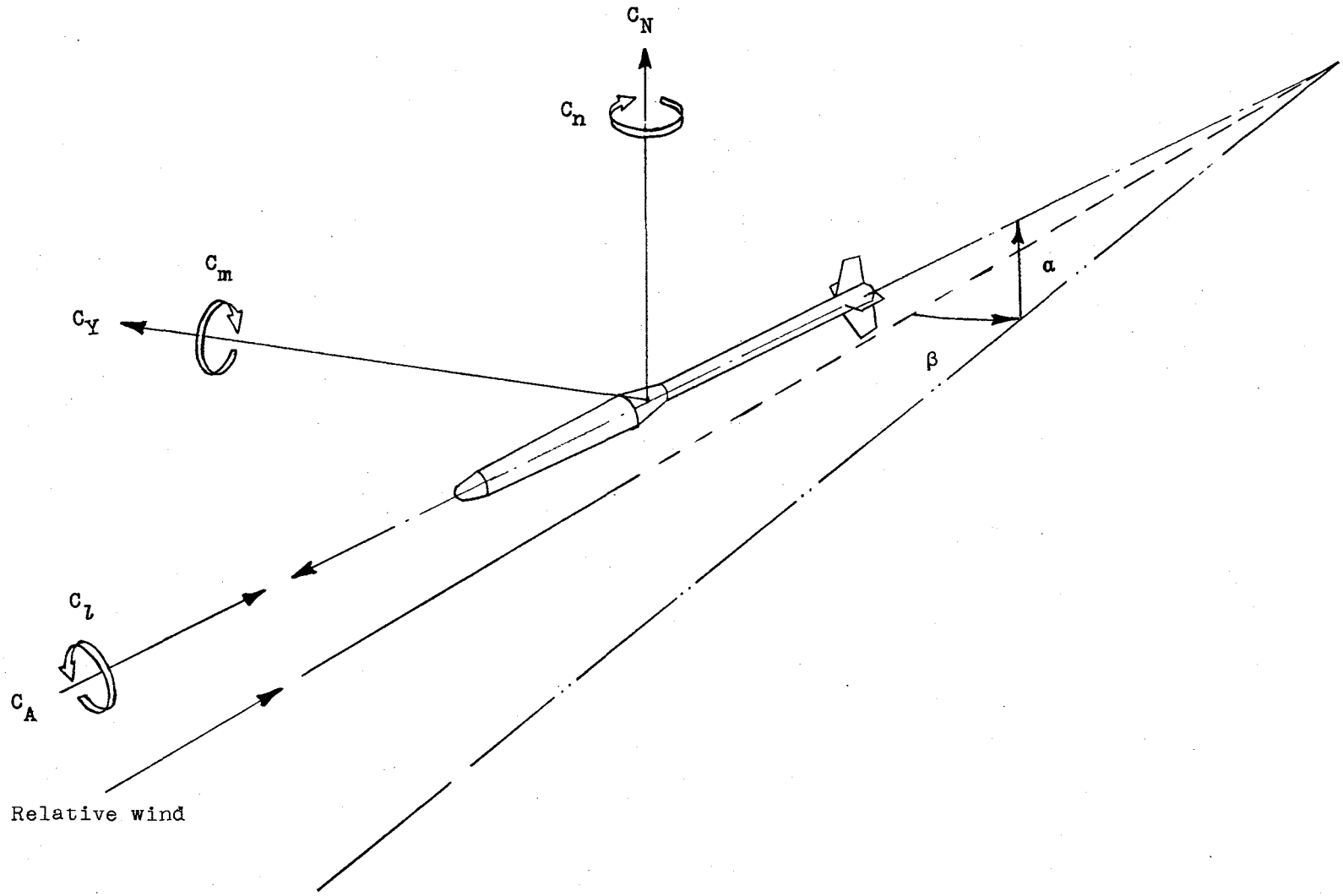

Figure 1.- Body-axis system. Arrows indicate positive direction.

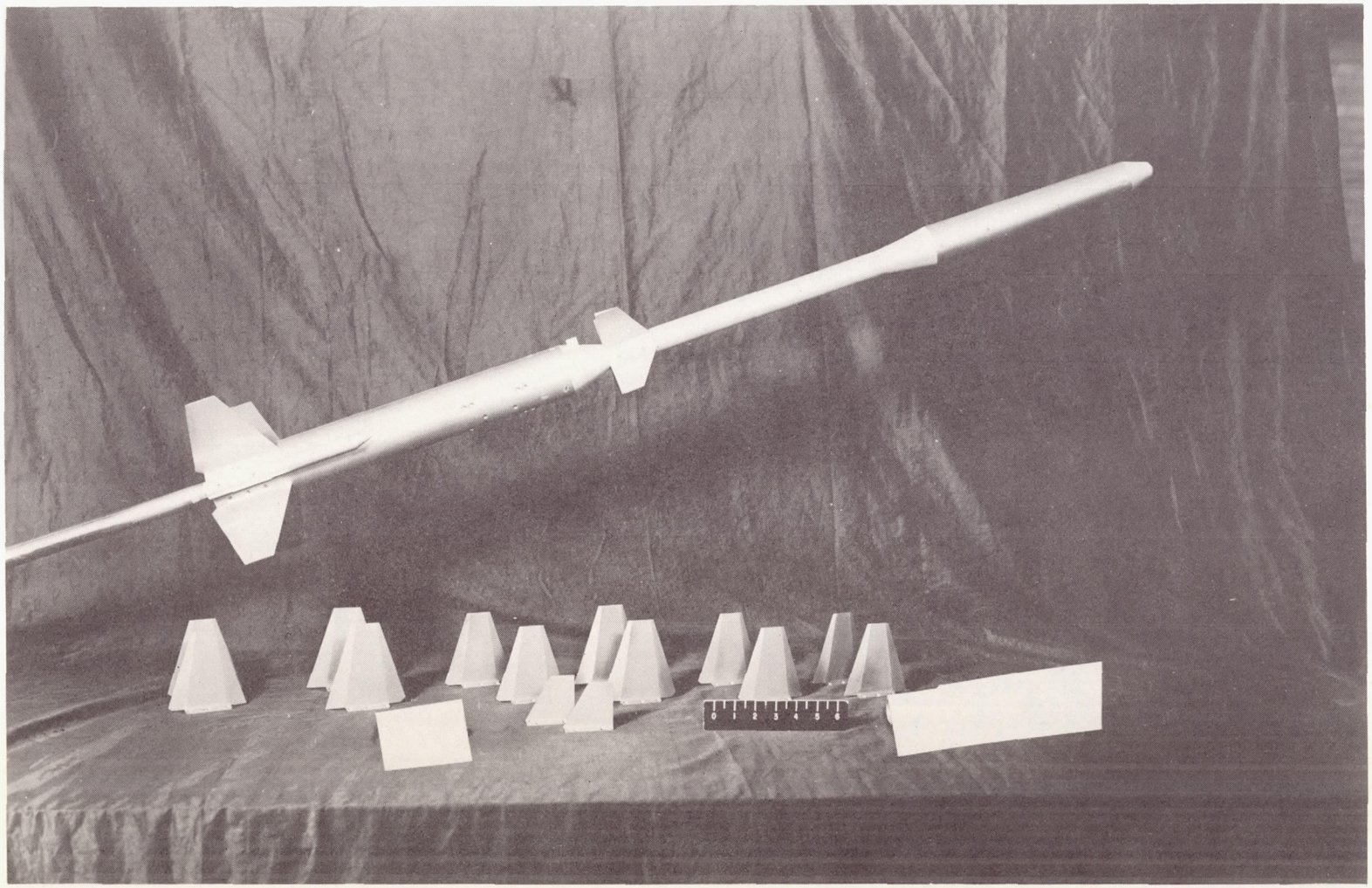

(a) Side view. L-60-7279.1

Figure 2.- Photographs of three-stage model of Trailblazer II configuration tested.

L-60-7280

(b) Plan view.

Figure 2.- Concluded.

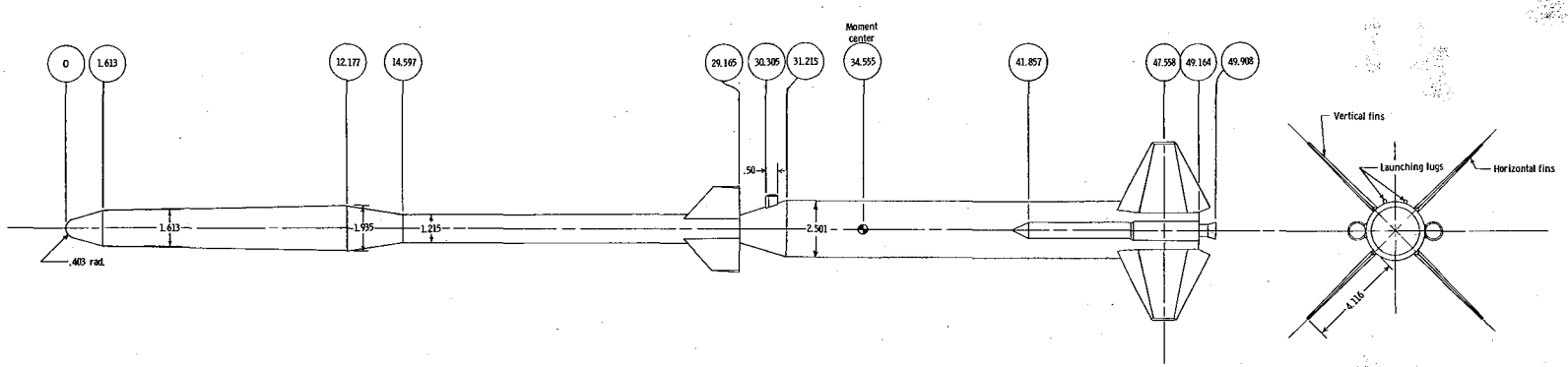

Figure 3.- Sketch of three-stage Trailblazer II configuration tested. All dimensions are in inches.

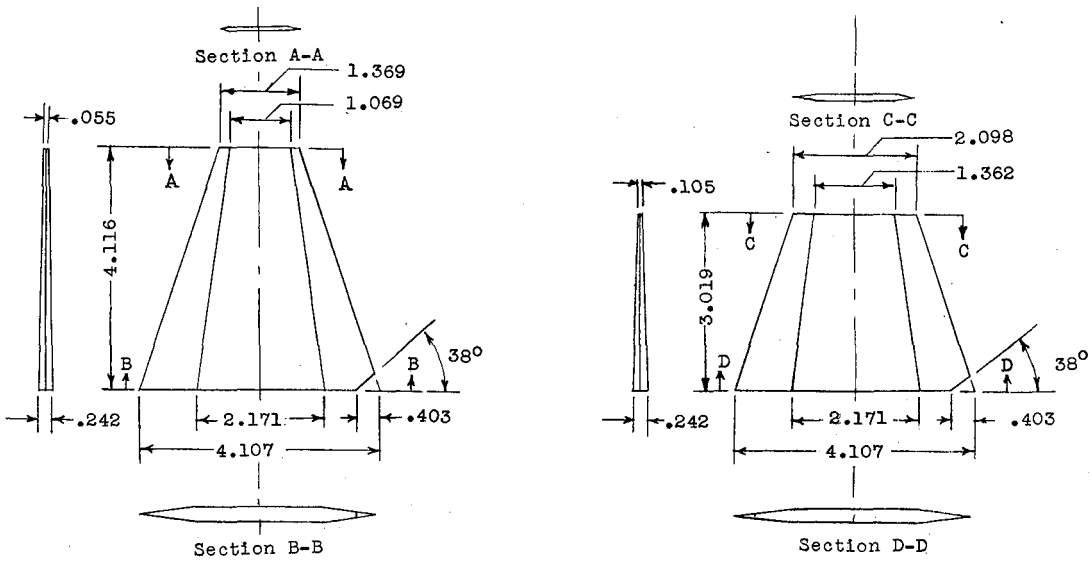

12-sq-ft, A = 1.5 fins

10-sq-ft, A = 0.985 fins

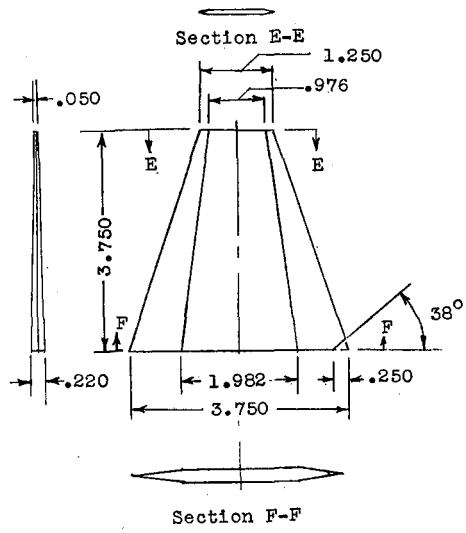

10-sq-ft, A = 1.5 fins

Figure 4.- Sketch of 0.081-scale models of first-stage booster fins. All dimensions are in inches unless otherwise noted.

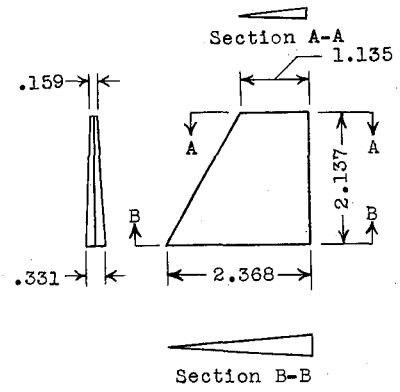

4-sq-ft fins

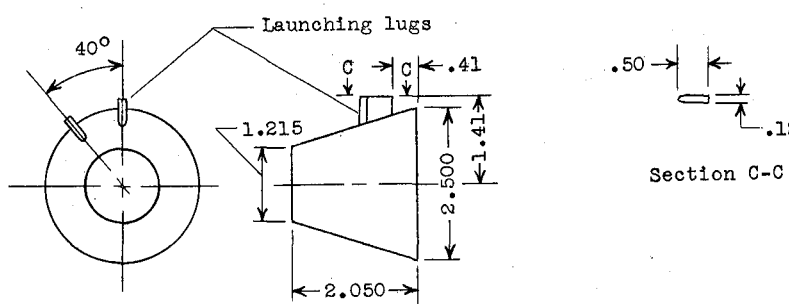

First-stage adapter

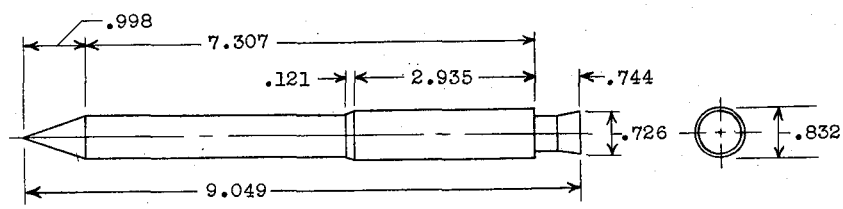

First-stage auxiliary rocket motor

Figure 5.- Sketch of second-stage booster fins, first-stage adapter, and first-stage auxiliary rocket motor. All dimensions are in inches unless otherwise noted.

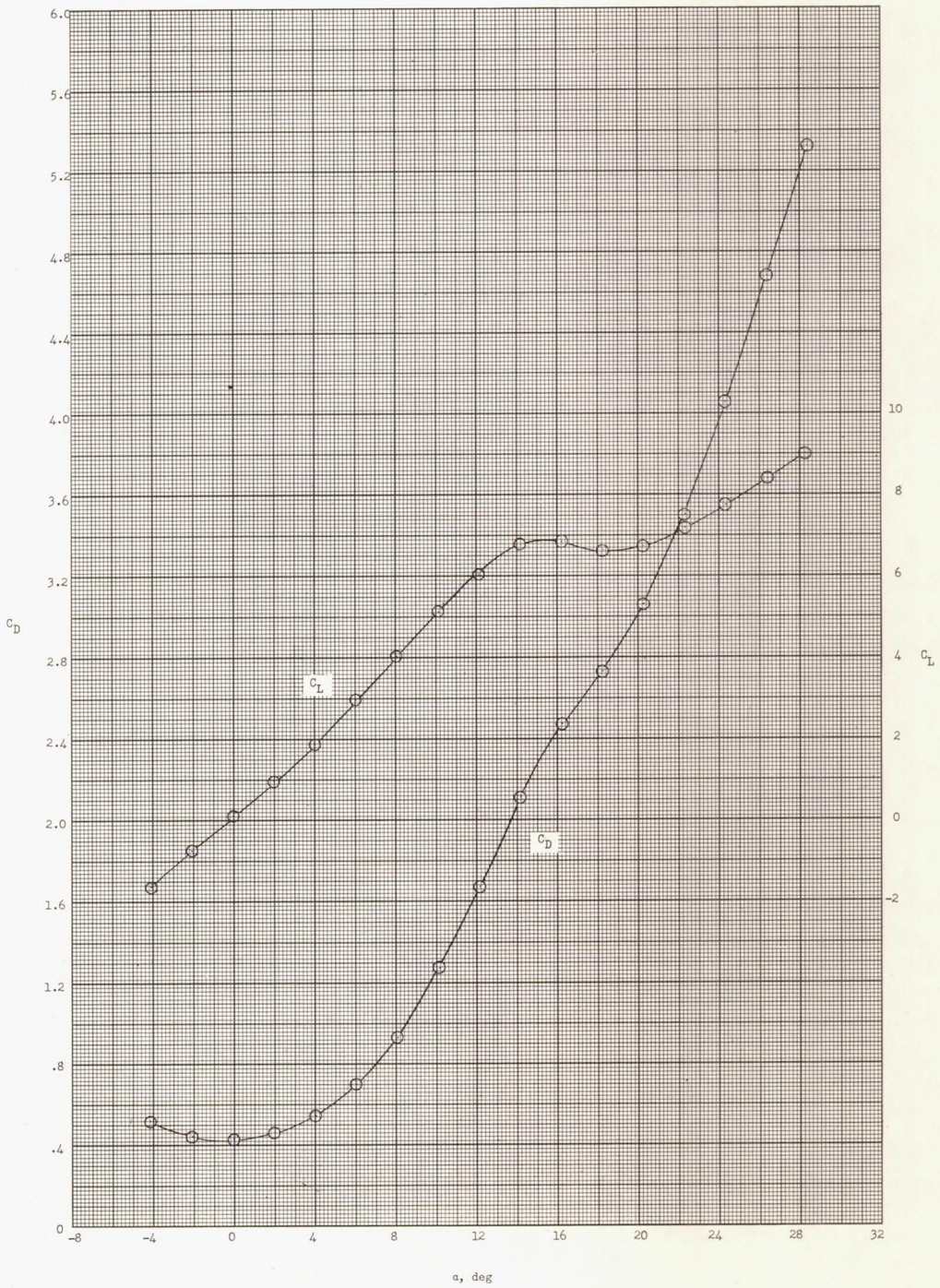

(a) Variation of C_L and C_D with α.

Figure 6.- Longitudinal aerodynamic characteristics of Trailblazer II configuration with 12-sq-ft, A = 1.5 fins. M = 0.205; R = 7.06×10^6.

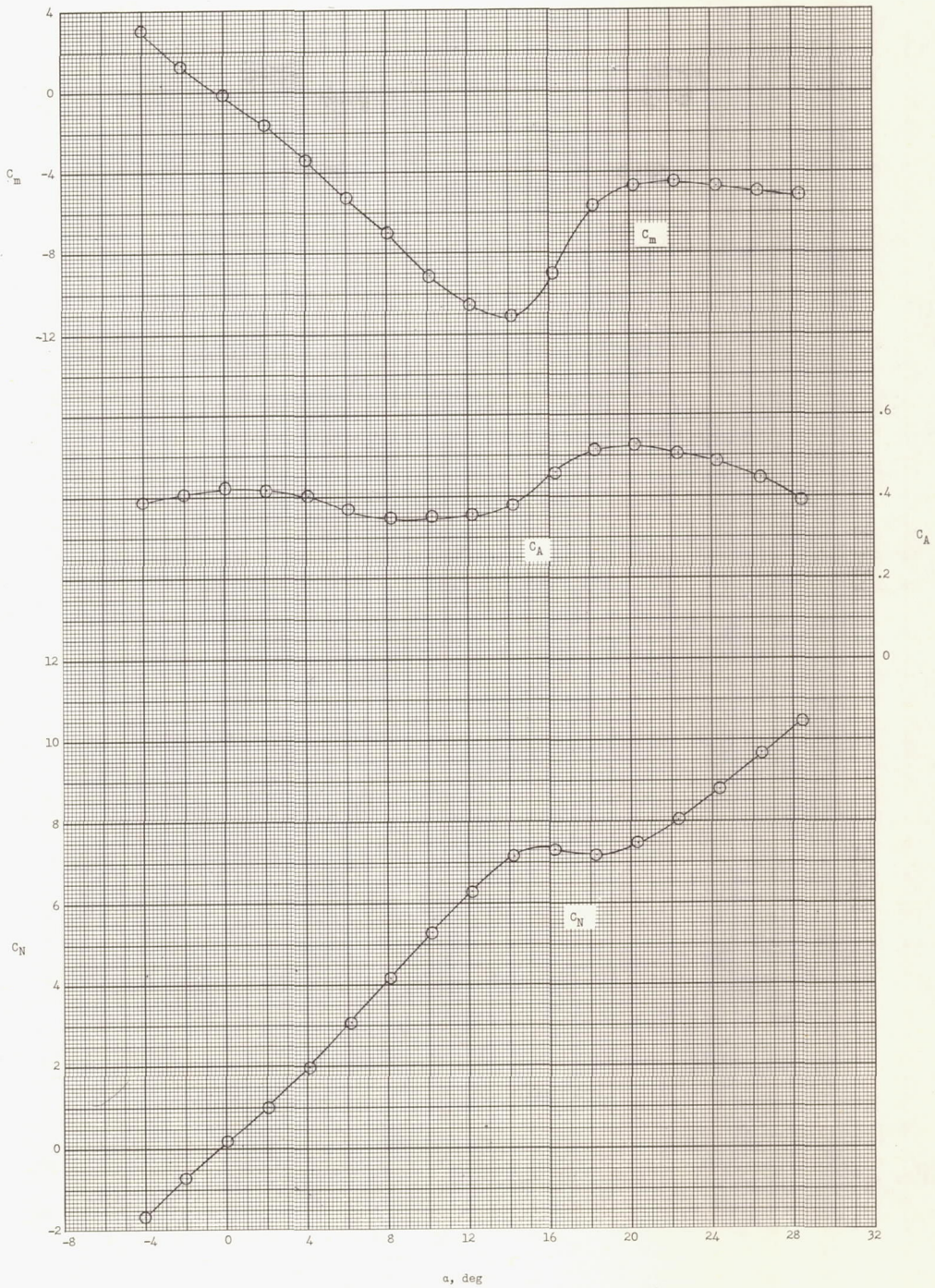

(b) Variation of C_m, C_A, and C_N with α.

Figure 6.- Concluded.

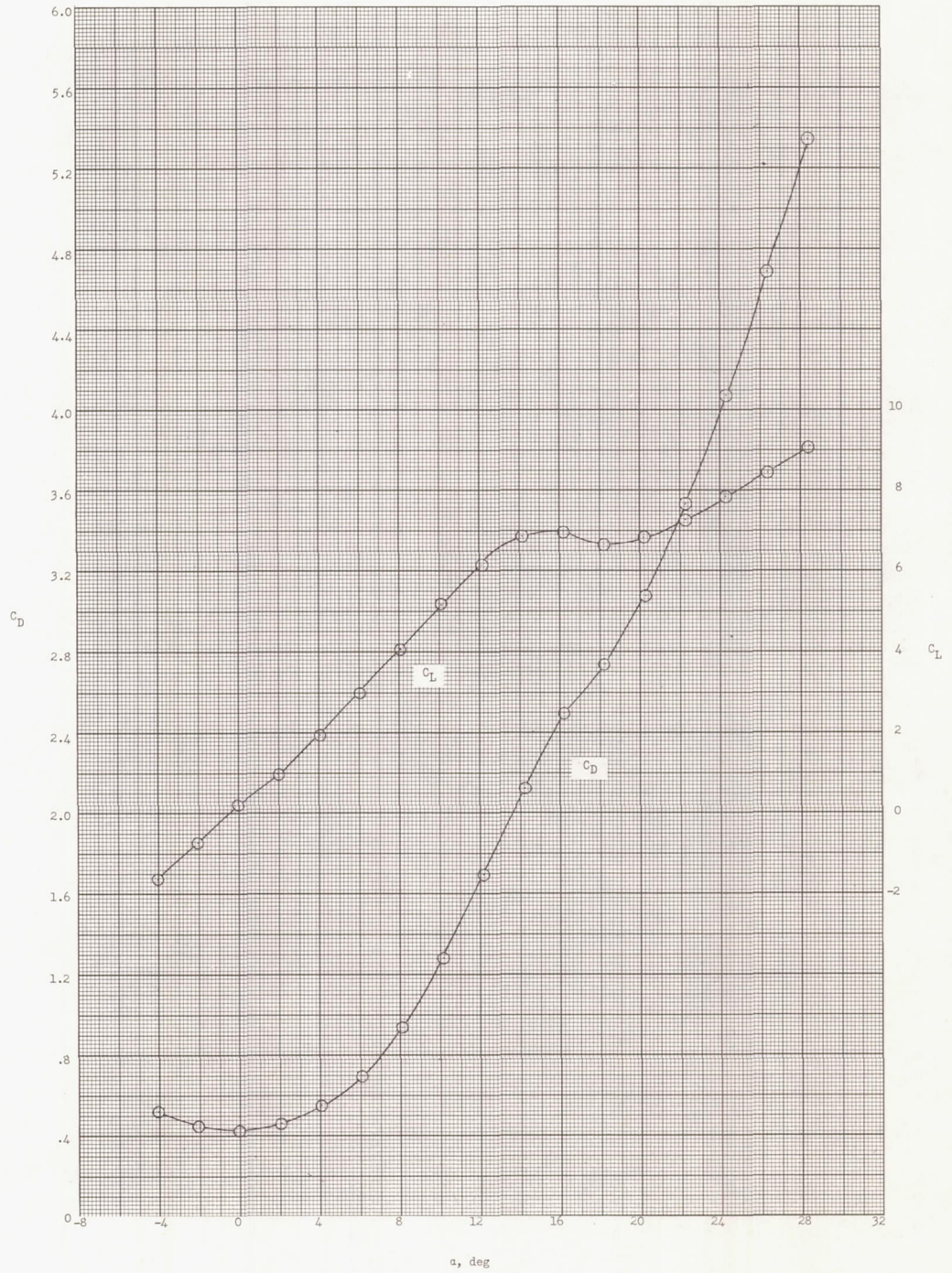

(a) Variation of C_L and C_D with α.

Figure 7.- Longitudinal aerodynamic characteristics of Trailblazer II configuration with 12-sq-ft, A = 1.5 fins. M = 0.156; R = 9.01×10^6.

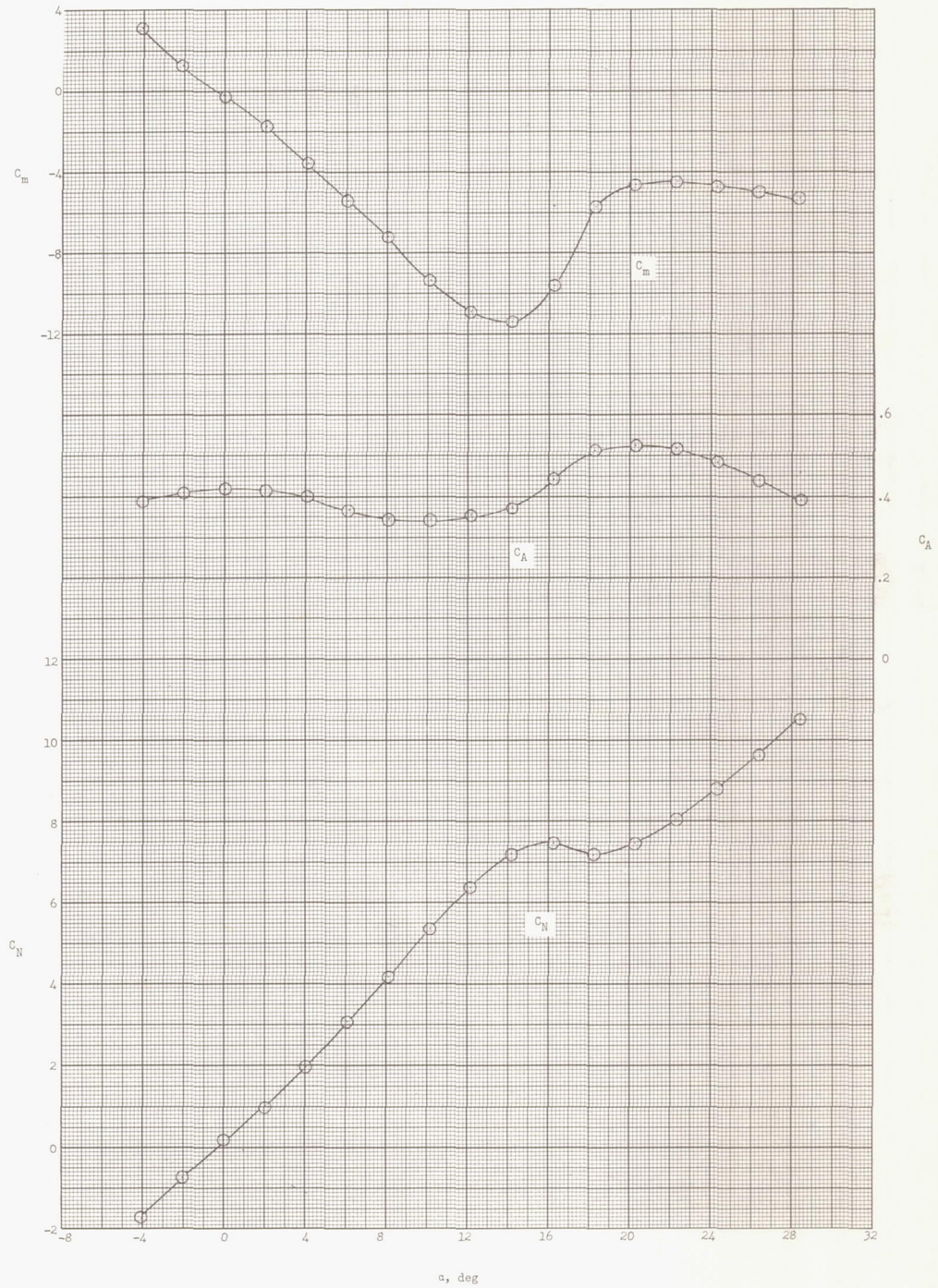

(b) Variation of C_m, C_A, and C_N with α.

Figure 7.- Concluded.

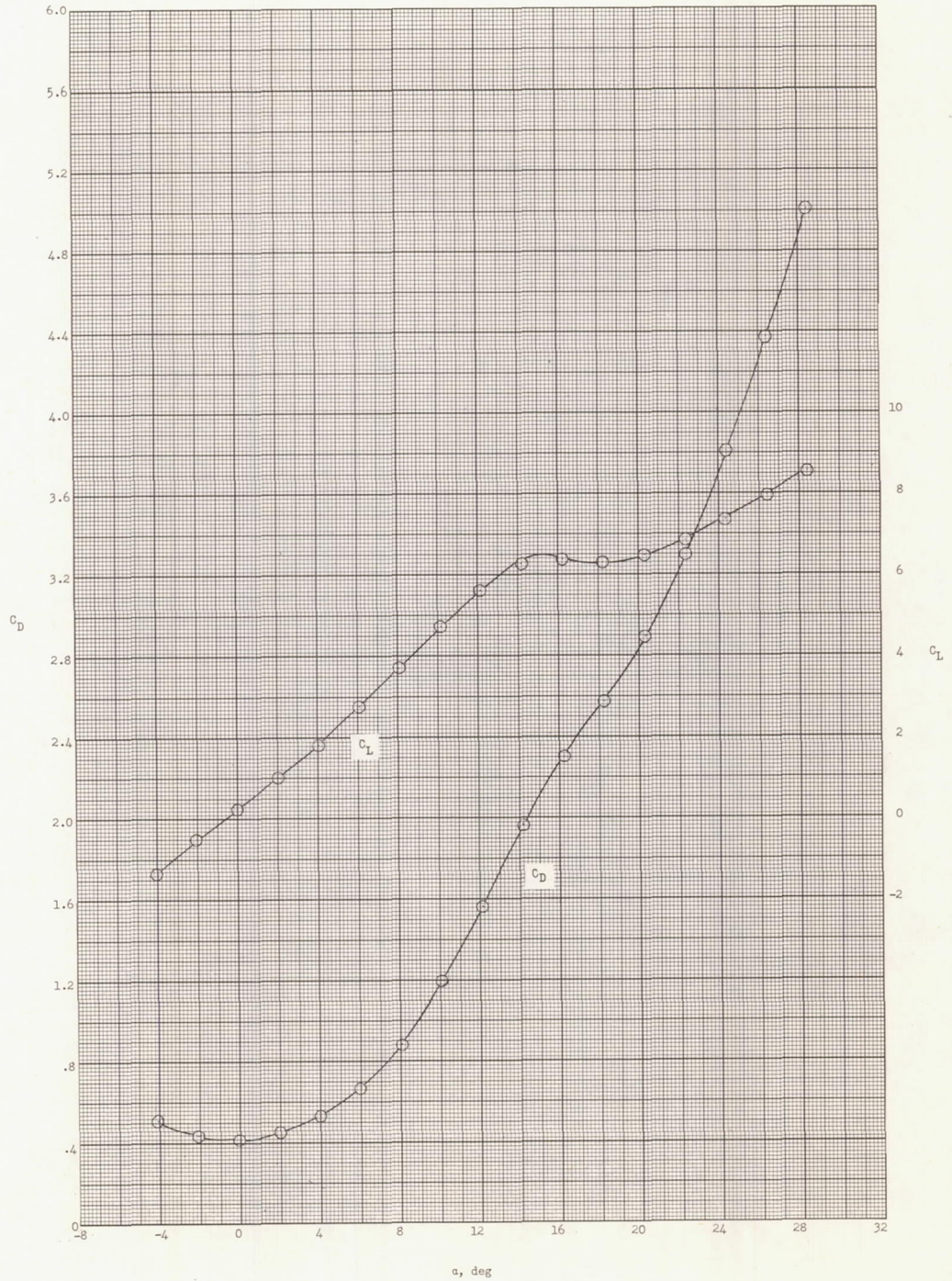

(a) Variation of C_L and C_D with α.

Figure 8.- Longitudinal aerodynamic characteristics of Trailblazer II configuration with 10-sq-ft, A = 1.5 fins. M = 0.161; R = 9.00×10^6.

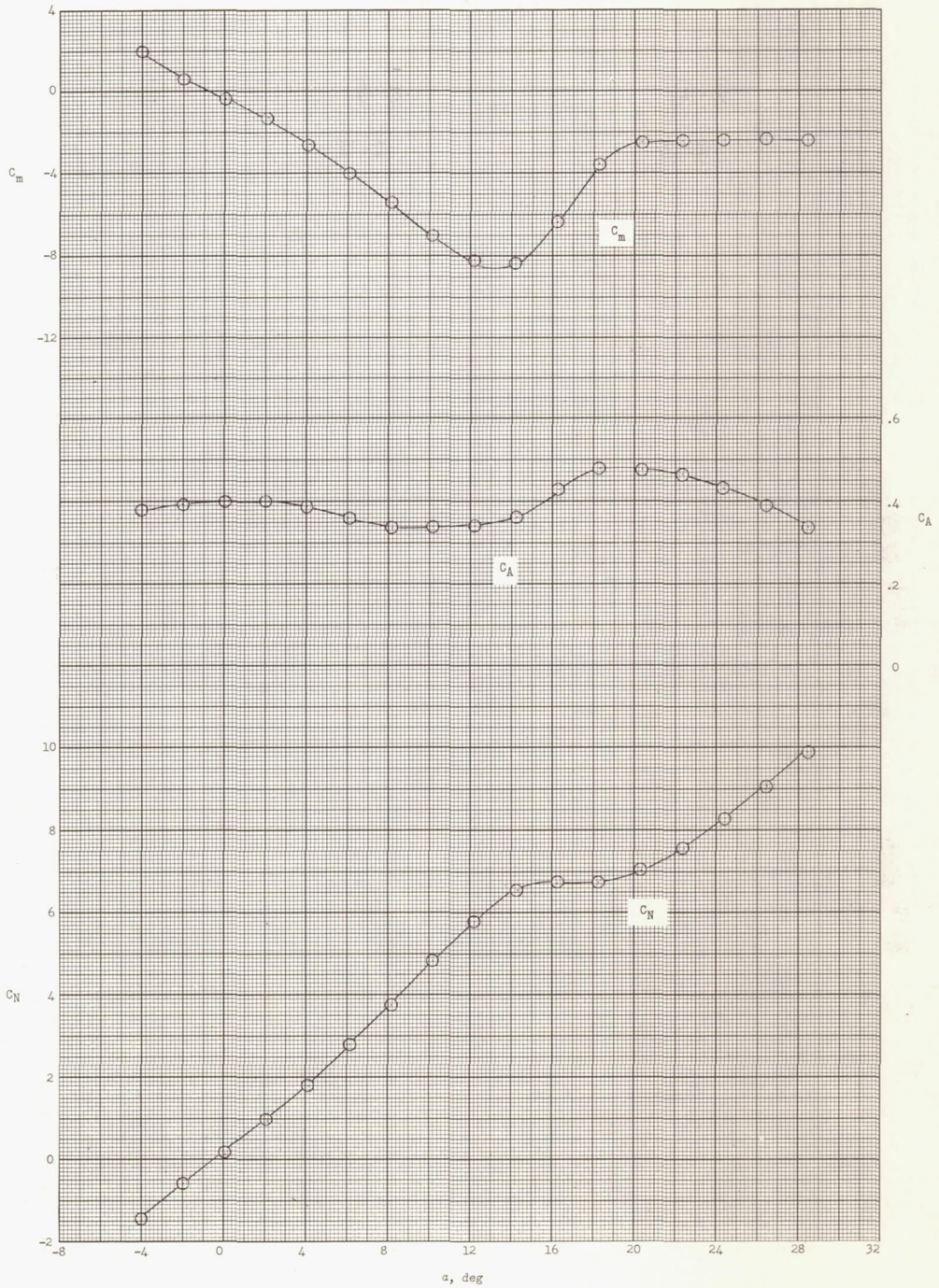

(b) Variation of C_m, C_A, and C_N with α.

Figure 8.- Concluded.

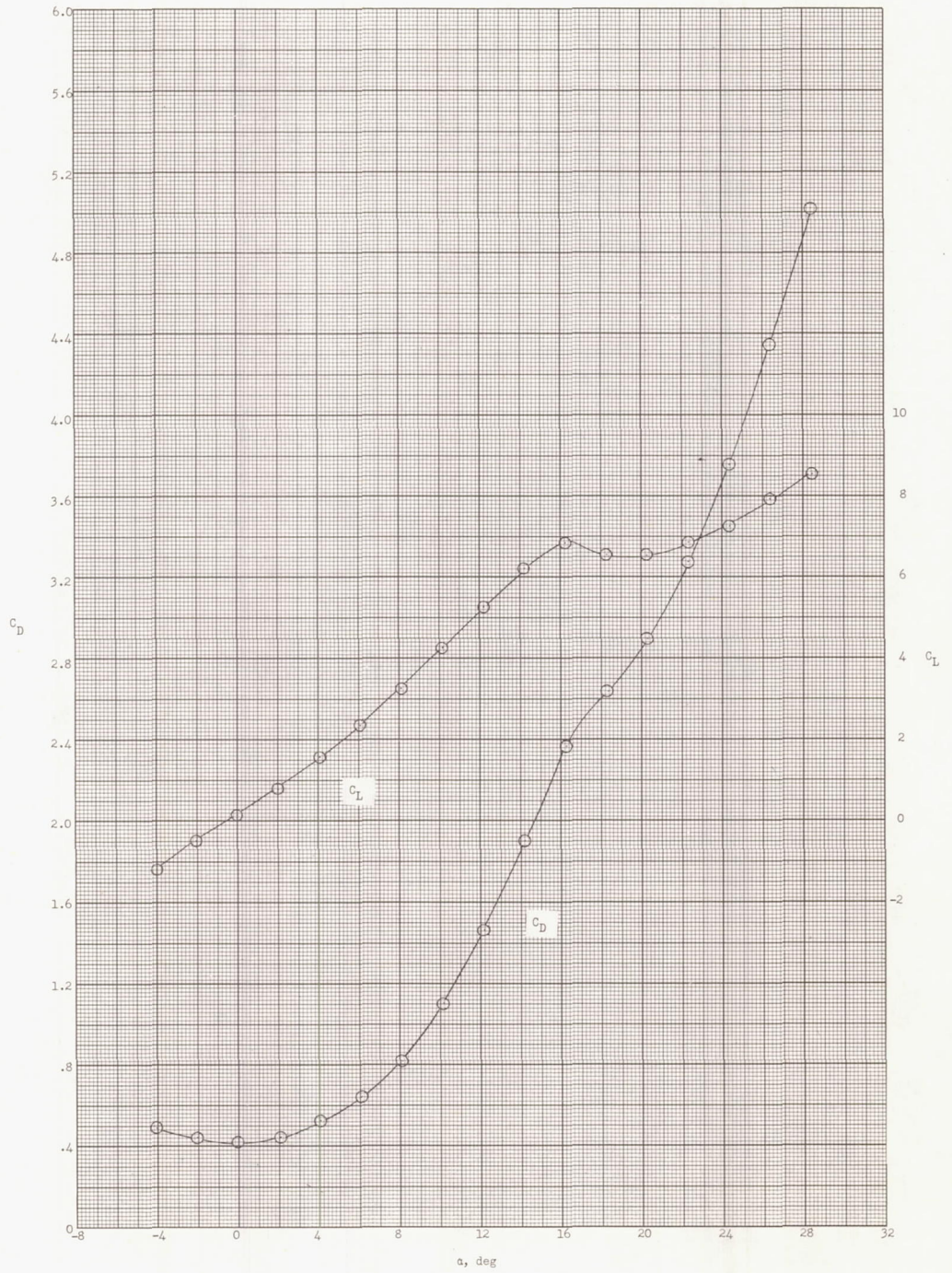

(a) Variation of C_L and C_D with α.

Figure 9.- Longitudinal aerodynamic characteristics of Trailblazer II configuration with 10-sq-ft, A = 0.985 fins. M = 0.159; R = 8.88×10^6.

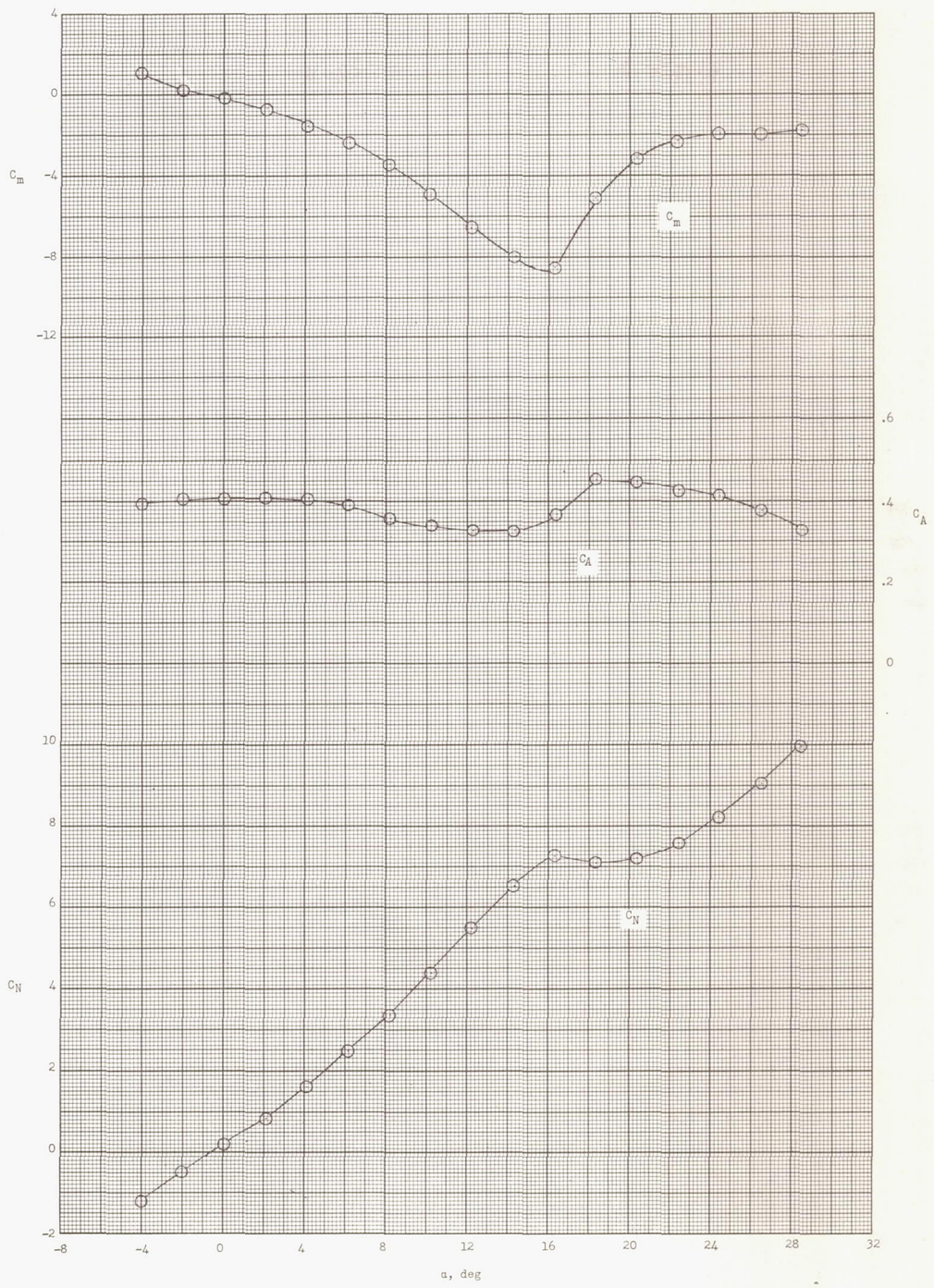

(b) Variation of C_m, C_A, and C_N with α.

Figure 9.- Concluded.

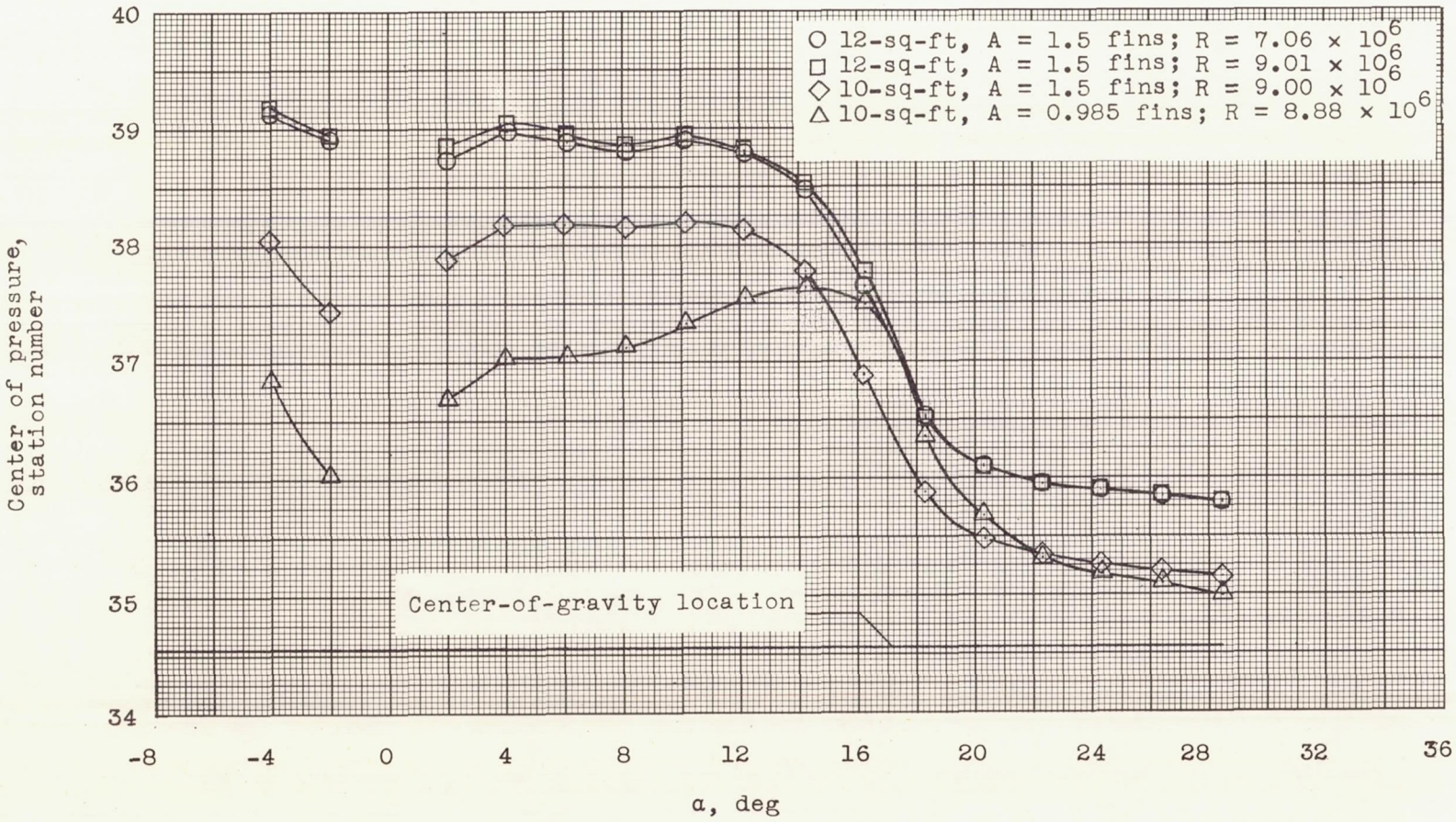

Figure 10.- Variation of the center-of-pressure location with angle of attack for all configurations tested.

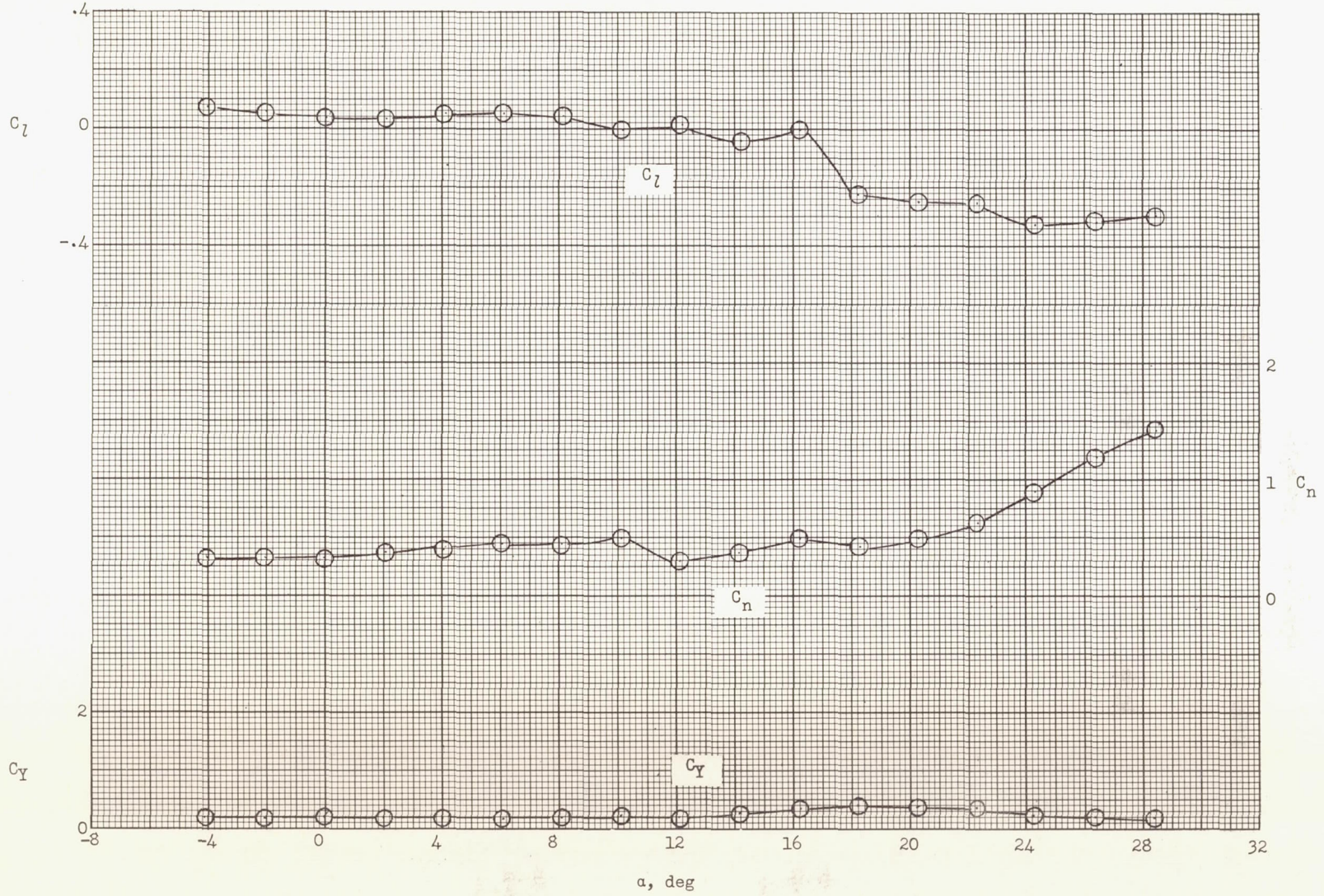

(a) 12-sq-ft, A = 1.5 fins. M = 0.205; R = 7.06×10^6.

Figure 11.- Lateral aerodynamic characteristics of Trailblazer II configuration at $\beta = 0^o$.

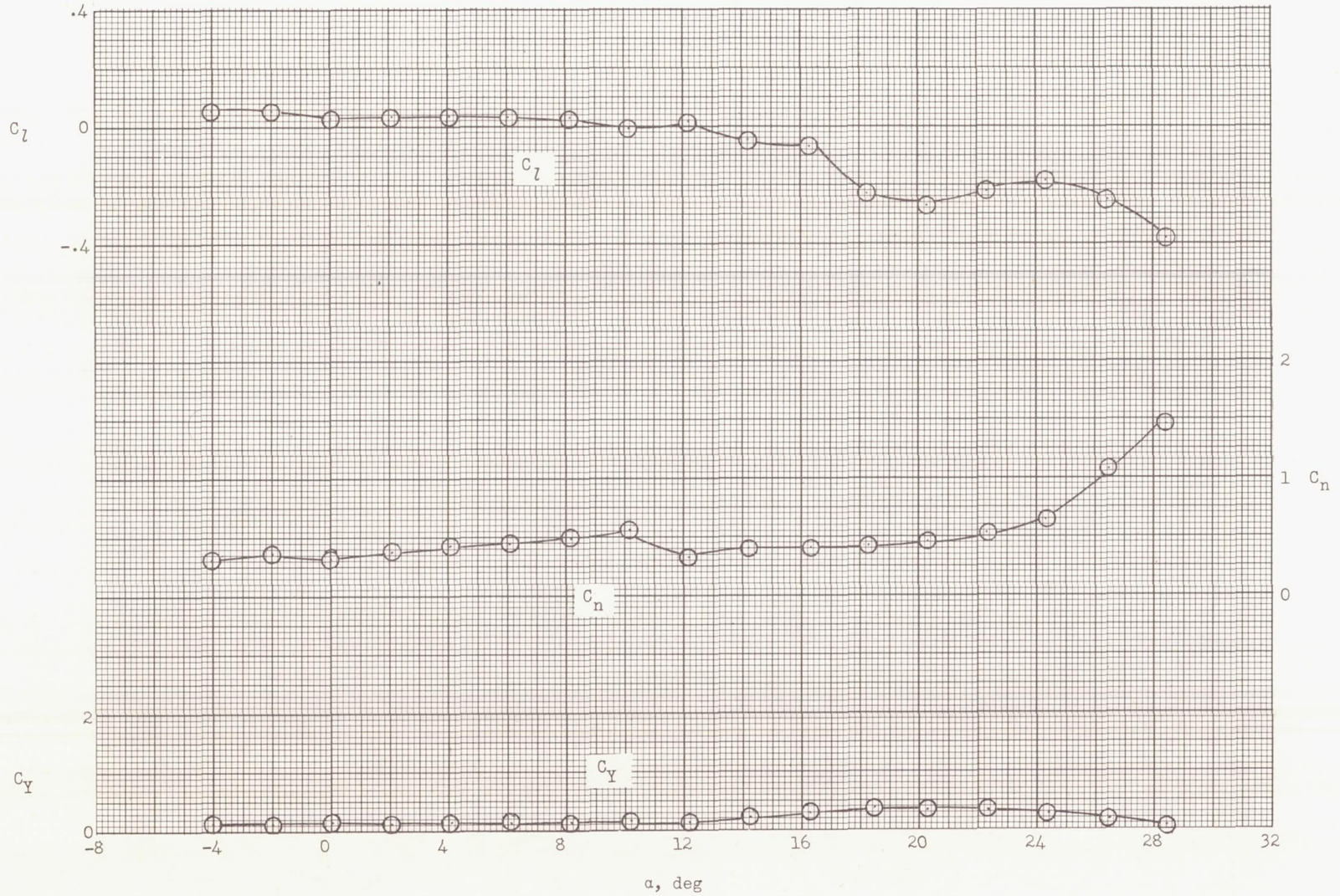

(b) 12-sq-ft, A = 1.5 fins. M = 0.156; R = 9.01×10^6.

Figure 11.- Continued.

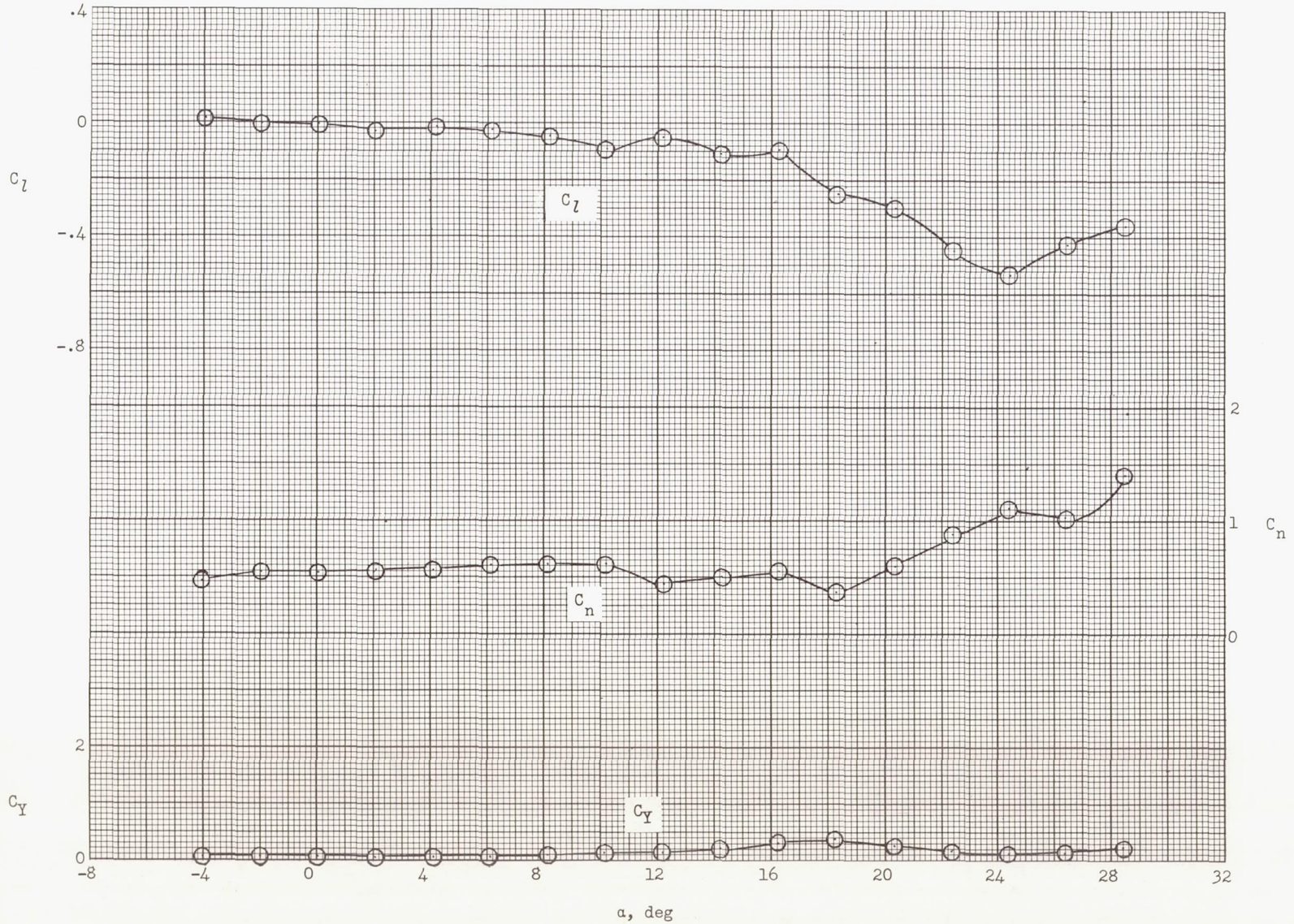

(c) 10-sq-ft, A = 1.5 fins. M = 0.161; R = 9.00×10^6.

Figure 11.- Continued.

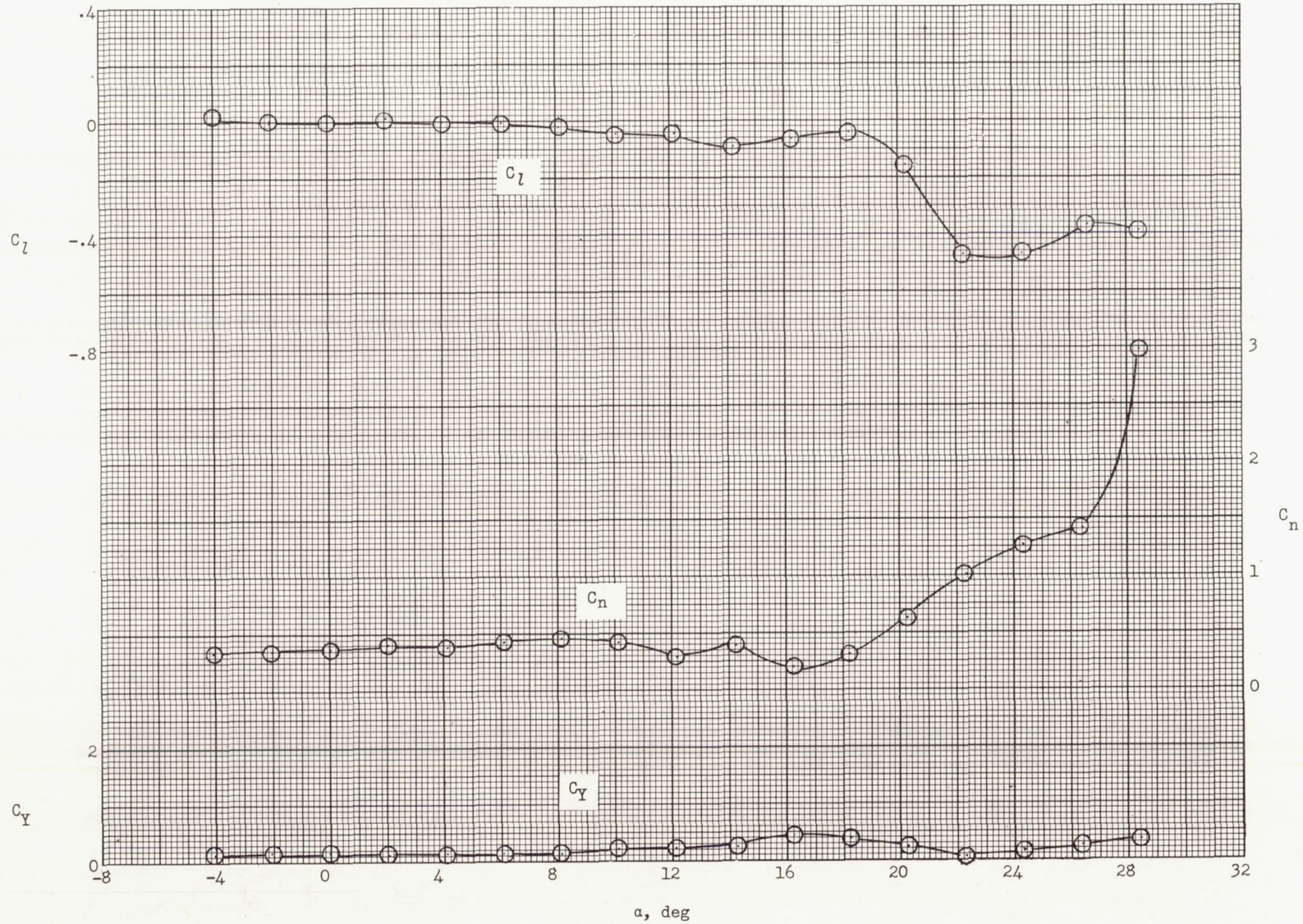

(d) 10-sq-ft, A = 0.985 fins. M = 0.159; R = 8.88×10^6.

Figure 11.- Concluded.